PRAMANA
— journal of
physics



Vol. 75, No. 4
October 2010
pp. 665–674

# $\omega(\rightarrow \pi^+\pi^-\pi^0)$ meson photoproduction on proton

SWAPAN DAS
Nuclear Physics Division, Bhabha Atomic Research Centre, Mumbai 400 085, India
E-mail: swapand@barc.gov.in

MS received 26 October 2009; revised 13 May 2010; accepted 14 May 2010

**Abstract.** The cross-section for the $\pi^+\pi^-\pi^0$ invariant mass distribution in the $\gamma p$ reaction in the GeV region is calculated. This reaction is assumed to proceed through the formation of the $\omega$-meson in the intermediate state, because the production cross-section for this meson in the $\gamma p$ reaction in the GeV region is significant and it has a large branching ratio (88.8%) in the $\pi^+\pi^-\pi^0$ channel. The cross-sections for this reaction are calculated using the energy-dependent reaction amplitude, $f_{\gamma p\rightarrow\omega p}(0)$, extracted from the latest $\omega$-meson photoproduction data. We use established procedure to calculate other factors, like width and propagator of the $\omega$-meson, so that our calculation can provide reliable cross-section. The calculated results reproduce the measured $\pi^+\pi^-\pi^0$ invariant mass distribution spectra in the $\gamma p$ reaction.

**Keywords.** $\omega$-meson production; $\gamma p$ reaction; $\pi^+\pi^-\pi^0$ invariant mass distribution.

**PACS No. 25.20.Lj**

## 1. Introduction

The vector meson production in the nuclear and particle reactions attracted growing interest over the years, as it revealed many rewarding physics in various topics of the hadronic physics. The importance of the vector meson in the context of pion production in the GeV region was realized long back [1–3]. The dilepton production in this energy region is due to the production of vector mesons in the intermediate state [4,5]. The vector dominance model (VDM) gives special status to the vector meson in describing the electromagnetic interaction between the lepton and hadron [6]. The vector meson can probe the low-lying nucleonic resonances [7] because it couples to these resonances through the tail of its mass distribution. The vector meson production process can be used to search for the missing resonances also [8]. For the latter purpose, the $\omega p$ system is preferred because of the narrow width (i.e., 8.43 MeV) of the $\omega$-meson. Of course, this system can only identify the nucleonic resonance of isospin $I = \frac{1}{2}$.

The vector meson has a significant role in understanding the quark-gluon picture of the hadron, because the quantum chromodynamics (QCD) describes it as a spin-triplet bound state of the specific valence quark ($q$) and antiquark ($\bar{q}$) pair in

the sea of $q\bar{q}$ pairs of all flavours including gluons. Indeed, the static quark picture (a simplified picture elucidating the vector meson as a spin triplet bound state of the specific $q\bar{q}$ pair only) [9] is deceptively successful in explaining some properties of the vector meson, such as spin-isopin for this meson, decay of vector meson, the potential energy between the $q\bar{q}$ pair, etc. In the energy region of hard scattering, the fluctuation of the quark-gluon configuration inside a hadron can be studied by the vector meson production process. This fluctuation makes better transparency (called colour transparency) for the vector meson propagation through the nucleus [10].

Recently, CBELSA/TAPS Collaboration at ELSA has done experiment for the $\omega$-meson photoproduction on proton and nuclear targets [11]. In this measurement, the $\omega$-meson was probed by the $\pi^0\gamma$ invariant mass distribution spectrum. We studied the mechanism for this reaction and calculated its cross-section [12]. It should be mentioned that the $\omega$-meson has only 8.5% branching ratio in the $\pi^0\gamma$ channel whereas it dominantly (88.8%) decays into the $\pi^+\pi^-\pi^0$ channel. Therefore, we calculate the cross-section for the $\pi^+\pi^-\pi^0$ invariant mass distribution (because it gives better signal for the $\omega$ meson production) in the $\gamma p$ reaction. We assume that this reaction proceeded as $\gamma p \to \omega p$; $\omega \to \pi^+\pi^-\pi^0$. To describe the $\omega$-meson photoproduction in the intermediate state, we extracted the energy-dependent $\gamma p \to \omega p$ reaction amplitudes from the latest measurement of the four-momentum transfer distributions (elaborated later). We followed the widely used procedure to evaluate all other factors appearing in the cross-section (e.g., the propagator and width of the $\omega$ meson) to get a reliable cross-section for the $\pi^+\pi^-\pi^0$ invariant mass distribution in the above mentioned reaction.

The formalism for this reaction is described in §2. The calculated results (along with the data) are described in §3. The conclusion of this study is presented in §4.

## 2. Formalism

The differential cross-section for the $\pi^+\pi^-\pi^0$ invariant mass distribution in the reaction: $\gamma p \to \omega p$; $\omega \to \pi^+\pi^-\pi^0$ can be expressed as

$$\frac{\mathrm{d}\sigma(m, E_\gamma)}{\mathrm{d}m} = \int \mathrm{d}\Omega_\omega [\mathrm{KF}] \Gamma_{\omega\to 3\pi}(m) |G_\omega(m)|^2 |F(\gamma p \to \omega p')|^2, \tag{1}$$

where [KF] represents the kinematical factor for the above reaction. It is given by

$$[\mathrm{KF}] = \frac{1}{(2\pi)^3} \frac{k_\omega^2 m_\mathrm{p} m^2}{k_\gamma |k_\omega (E_\gamma + m_\mathrm{p}) - \mathbf{k}_\gamma \cdot \hat{\mathbf{k}}_\omega E_\omega|}. \tag{2}$$

All symbols carry their usual meanings.

$\Gamma_{\omega\to 3\pi}(m)$ in eq. (1) denotes the width for $\omega$ (at rest) $\to \pi^+\pi^-\pi^0$, i.e., $\Gamma_{\omega\to 3\pi}(m) \equiv \Gamma_{\omega\to\pi^+\pi^-\pi^0}$, governed by the Lagrangian density $\mathcal{L}_{\omega 3\pi} = \frac{f_{\omega 3\pi}}{m_\pi^3} \epsilon_{\mu\nu\lambda\sigma} \omega^\mu k_{\pi^+}^\nu k_{\pi^-}^\lambda k_{\pi^0}^\sigma$ [13]. The expression for $\Gamma_{\omega\to\pi^+\pi^-\pi^0}$ is given in eq. (5). The $\omega$-meson propagator $G_\omega^{\mu\mu'}(m)$ is given by $G_\omega^{\mu\mu'}(m) = (-g^{\mu\mu'} + \frac{1}{m^2} k_\omega^\mu k_\omega^{\mu'}) G_\omega(m)$. $g^{\mu\mu'}$ couples the $\pi^+\pi^-\pi^0$ field (in the final state) to the vector field. The second

part of the propagator does not contribute because of the antisymmetric coupling of $\omega$-meson to three pions (see the equation for $\mathcal{L}_{\omega 3\pi}$, given earlier). The factor $G_\omega(m)$, which also appears in eq. (1), describes the scalar part of the $\omega$-meson propagator in the free space. The expression for $G_\omega(m)$ is

$$G_\omega(m) = \frac{1}{m^2 - m_\omega^2 + i m_\omega \Gamma_\omega(m)}, \tag{3}$$

where $m_\omega \simeq 782$ MeV. $\Gamma_\omega(m)$ denotes the total free space decay width for the $\omega$-meson. It is composed of hadronic, semi-hadronic and leptonic decay channels [14]:

$$\begin{aligned}\Gamma_\omega(m) \approx{}& \Gamma_{\omega\to\pi^+\pi^-\pi^0}(88.8\%) + \Gamma_{\omega\to\pi^0\gamma}(8.5\%) \\ &+ \Gamma_{\omega\to\pi^+\pi^-}(2.21\%) + \Gamma_{\omega\to l^+l^-}(\sim 10^{-4}\%).\end{aligned} \tag{4}$$

The leptonic decay channels (i.e., $\Gamma_{\omega\to l^+l^-}$) for the $\omega$-meson are insignificant when compared with other decay channels, and so they are ignored in this calculation.

The form for $\Gamma_{\omega\to\pi^+\pi^-\pi^0}(m)$ in eq. (4), as shown by Sakurai [13], is given by

$$\Gamma_{\omega\to\pi^+\pi^-\pi^0}(m) = \Gamma_{\omega\to\pi^+\pi^-\pi^0}(m_\omega)\frac{m}{m_\omega}\frac{(m-3m_\pi)^4}{(m_\omega-3m_\pi)^4}\frac{U(m)}{U(m_\omega)}, \tag{5}$$

with $\Gamma_{\omega\to\pi^+\pi^-\pi^0}(m_\omega \simeq 782\text{ MeV}) \simeq 7.49$ MeV [14]. The function $U(m)$ is described in ref. [13] as $U(m) \to 1$ for $m \to 3m_\pi$ and $U(m) \to 1.6$ for $m \to 787$ MeV. It is also taken equal to 1.6 for $m > 787$ MeV.

The width $\Gamma_{\omega\to\pi^0\gamma}(m)$ appearing in eq. (4) is evaluated using the Lagrangian density: $\mathcal{L}_{\omega\pi^0\gamma} = (f_{\omega\pi\gamma}/m_\pi)\epsilon_{\mu\nu\rho\sigma}\partial^\mu A^\nu \pi^0 \partial^\rho \omega^\sigma$ [15]. The expression for this is

$$\Gamma_{\omega\to\pi^0\gamma}(m) = \Gamma_{\omega\to\pi^0\gamma}(m_\omega)\left[\frac{k(m)}{k(m_\omega)}\right]^3, \tag{6}$$

where $\Gamma_{\omega\to\pi^0\gamma}(m_\omega) \simeq 0.72$ MeV at $m_\omega \simeq 782$ MeV [14] and $k(m)$ denotes the momentum of pion originating due to the $\omega$-meson of mass $m$ decaying at rest.

In eq. (4), $\Gamma_{\omega\to\pi^+\pi^-}(m)$ denotes the width of the $\omega$-meson decaying to $\pi^+\pi^-$ channel. In fact, this channel arises due to the small isovector component present in the physical $\omega$-meson, i.e., $\omega = \omega_{\rm I}(0,0) + \epsilon\rho_{\rm I}(1,0)$ [5]. Here, $\omega_{\rm I}(0,0)$ and $\rho_{\rm I}(1,0)$ denote the isoscaler and isovector fields respectively. $\epsilon$ is the small mixing parameter. Therefore, the isovector $\pi^+\pi^-$ current can strongly couple to $\rho_{\rm I}(1,0)$ in the Lagrangian density $\mathcal{L}_{\omega\pi\pi} = f_{\omega\pi\pi}(\vec{\pi}\times\partial_\mu\vec{\pi})\cdot\omega^\mu$ and $\omega_{\rm I}(0,0)$ can be ignored for this purpose. We do not use isovector sign on the $\omega$-meson appearing in the Lagrangian since the $\rho_{\rm I}(1,0)$ content in the $\omega$-meson is very small. In ref. [5] it has been clearly shown that even if $\omega_{\rm I}(0,0) \to \pi^+\pi^-$ is allowed due to charge symmetry violation (CSV), the $\pi^+\pi^-$ emission from the $\omega$-meson is possible only due to $\rho_{\rm I}(1,0) \to \pi^+\pi^-$ for $m_\rho \sim m_\omega$ and $\Gamma_\rho \gg \Gamma_\omega$. The width of the $\omega \to \pi^+\pi^-$ channel is given as

$$\Gamma_{\omega\to\pi^+\pi^-}(m) = \Gamma_{\omega\to\pi^+\pi^-}(m_\omega)\frac{m_\omega}{m}\left[\frac{k(m)}{k(m_\omega)}\right]^3. \tag{7}$$

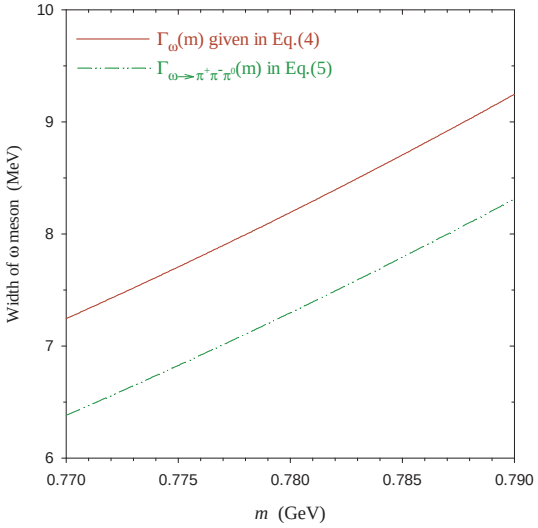


**Figure 1.** The dependence of $\Gamma_\omega(m)$ in eq. (4) and $\Gamma_{\omega\to\pi^+\pi^-\pi^0}(m)$ in eq. (5) on the $\omega$-meson mass.

The value for $\Gamma_{\omega\to\pi^+\pi^-}(m_\omega \simeq 782$ MeV), according to ref. [14], is approximately equal to 0.19 MeV. $k(m)$ represents the pion momentum in the $\pi^+\pi^-$ cm of the system.

The $\omega$-meson dominantly decays to $\pi^+\pi^-\pi^0$ channel (see $\Gamma_\omega(m)$ in eq. (4)). Therefore, the mass distribution of the $\omega$-meson is significantly governed by the decay width of this channel, i.e., $\Gamma_{\omega\to\pi^+\pi^-\pi^0}(m)$, expressed in eq. (5). The $\omega$-meson possesses narrow width (about 8.43 MeV) in the free space. To justify it, we plot the mass $m$ dependence of $\Gamma_\omega(m)$ in eq. (4) and $\Gamma_{\omega\to\pi^+\pi^-\pi^0}(m)$ in eq. (5) in figure 1. This figure shows that expressions used for these widths duly reproduce the respective measured values at $m = m_\omega$, quoted in ref. [14].

The generalized potential for the $\omega$-meson photoproduction in the nuclear reaction can be expressed as $F(\gamma p \to \omega p')\varrho(\mathbf{r})$ [16], where $\varrho(\mathbf{r})$ represents the density distribution of the target nucleus. For the point particle (i.e., proton target), the density distribution $\varrho(\mathbf{r}) = \delta(\mathbf{r})$. The form for $F(\gamma p \to \omega p')$, which appears in eq. (1), in the centre of mass system is given by

$$F(\gamma p \to \omega p') = -4\pi \left[1 + \frac{E_\omega}{E_{p'}}\right] f_{\gamma p\to\omega p'}(0), \tag{8}$$

where $f_{\gamma p\to\omega p'}(0)$ is the forward amplitude for the $\gamma p \to \omega p'$ reaction. In the cross-section in eq. (1), $f_{\gamma p\to\omega p'}(0)$ appears in the form of $|f_{\gamma p\to\omega p'}(0)|^2$ which is related to the four-momentum $q^2$ transfer distribution $\mathrm{d}\sigma(\gamma p \to \omega p')/\mathrm{d}q^2$ [17] as

$$\frac{\mathrm{d}\sigma}{\mathrm{d}q^2}(\gamma p \to \omega p'; q^2 = 0) = \frac{\pi}{k_\gamma^2}|f_{\gamma p\to\omega p'}(0)|^2. \tag{9}$$

$\mathrm{d}\sigma(\gamma p \to \omega p'; q^2 = 0)/\mathrm{d}q^2$ is used to be obtained from the extrapolation of the measured $\mathrm{d}\sigma(\gamma p \to \omega p'; q^2)/\mathrm{d}q^2$. In fact, its energy-dependent values are reported

in refs [17,18] for $E_\gamma \geq 1.6$ GeV. In the present study, we deal with the $\omega$-meson photoproduction for the beam energy range: $E_\gamma$(GeV) = 1.1–9.3. In the lower energy region, i.e., $E_\gamma \leq 2.6$ GeV, the data for the $\mathrm{d}\sigma(\gamma p \rightarrow \omega p')/\mathrm{d}q^2$ distribution are taken from the measurement (done recently) with the SAPHIR detector at electron stretcher ring (ELSA), Bonn [19]. In this measurement, the measured

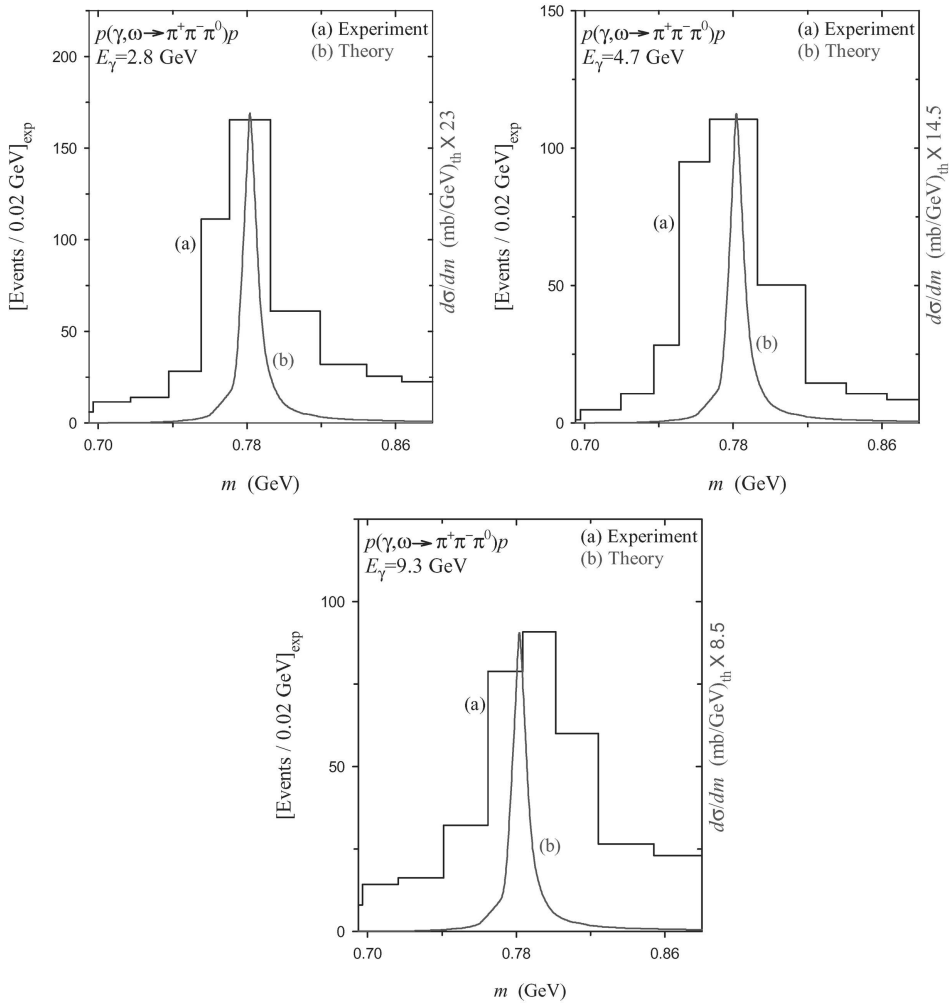


**Figure 2.** The calculated $\omega(\rightarrow \pi^+\pi^-\pi^0)$ meson mass distribution spectra for various beam (gamma) energies are presented. $m$ denotes the mass of the $\omega$-meson, i.e., the $\pi^+\pi^-\pi^0$ invariant mass in the measurement. The histograms (a) represent the $\pi^+\pi^-\pi^0$ invariant mass distribution spectra (along with the background <10%) measured by Ballam *et al* [2]. They are given in events/0.02 GeV. The solid curves (b) show the calculated results, i.e., $\mathrm{d}\sigma/\mathrm{d}m$ due to eq. (1). The calculated results are normalized to the measured spectra at the respective peaks.

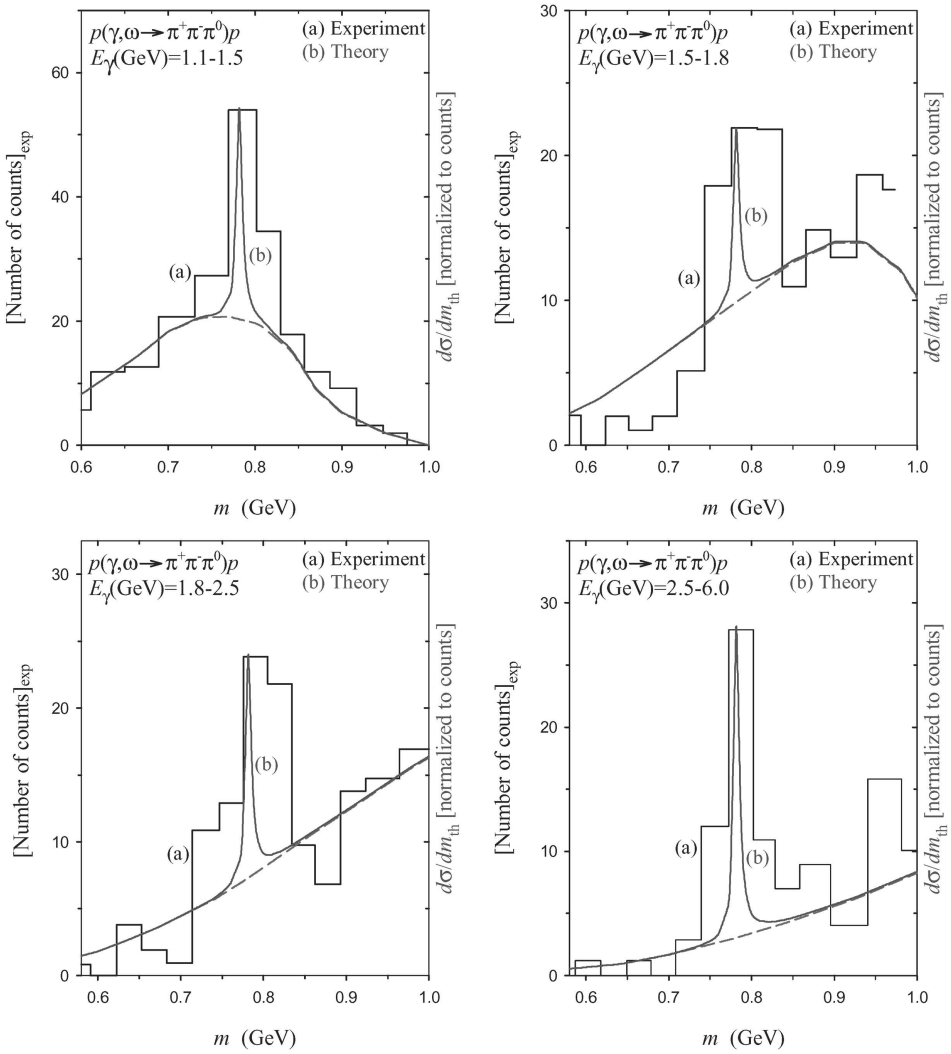


**Figure 3.** The calculated $\omega(\rightarrow \pi^+\pi^-\pi^0)$ meson mass distribution spectra are compared with the data due to BUBBLE chamber group [3]. In each energy bin, the histogram (a) represents the number of counts for the measured $\pi^+\pi^-\pi^0$ invariant mass distribution spectrum and the dashed curve describes the phase space [3]. The solid curves (b) are related to the calculated cross–section $\mathrm{d}\sigma/\mathrm{d}m$ in eq. (10), explained in the text.

$\mathrm{d}\sigma(\gamma p \rightarrow \omega p')/\mathrm{d}q^2$ vs. $|q^2 - q^2_{\mathrm{min}}|$ ($q^2_{\mathrm{min}}$ is defined in refs [17,20]) is reported. Therefore, we extract $|f_{\gamma p\rightarrow\omega p'}(0)|^2$ from the SAPHIR data for $E_\gamma \leq 2.6$ GeV. For $E_\gamma \geq 2.6$ GeV, the energy-dependent $|f_{\gamma p\rightarrow\omega p'}(0)|^2$ is evaluated from the forward $\mathrm{d}\sigma(\gamma p \rightarrow \omega p')/\mathrm{d}q^2$ given in refs [17,18].

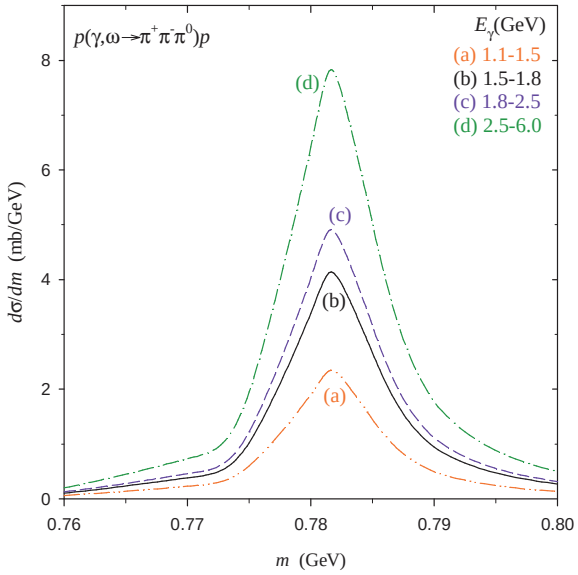


**Figure 4.** The calculated $\omega(\rightarrow \pi^+\pi^-\pi^0)$ meson mass distribution spectra for various beam (gamma) energy bins are presented. The curves appearing in this figure are the calculated results due to eq. (10). This figure distinctly shows the enhancement in the cross-section with the beam energy.

Equation (1) can be used to calculate the differential cross-section for the $\pi^+\pi^-\pi^0$ invariant mass distribution $\mathrm{d}\sigma(m, E_\gamma)/\mathrm{d}m$ due to $\omega \rightarrow \pi^+\pi^-\pi^0$ for a fixed beam energy $E_\gamma$. To describe this reaction for the $\gamma$ beam of certain energy range, as it happens for the tagged photon, we modulate the cross-section given in eq. (1) with the beam profile function $W(E_\gamma)$ [21], i.e.,

$$\frac{\mathrm{d}\sigma(m)}{\mathrm{d}m} = \int_{E_\gamma^{\min}}^{E_\gamma^{\max}} \mathrm{d}E_\gamma W(E_\gamma) \frac{\mathrm{d}\sigma(m, E_\gamma)}{\mathrm{d}m}. \tag{10}$$

The profile function $W(E_\gamma)$ for the $\gamma$ beam, originating because of the bremsstrahlung radiation of the electron, varies as $W(E_\gamma) \propto (1/E_\gamma)$ [21].

## 3. Results and discussion

We calculate the cross-sections $\mathrm{d}\sigma/\mathrm{d}m$ for the $\omega(\rightarrow \pi^+\pi^-\pi^0)$ meson mass distribution spectra using eq. (1) for beam energies ($E_\gamma$ in GeV) 2.8, 4.7 and 9.3. The calculated results (solid curves) are compared in figure 2 with the $\pi^+\pi^-\pi^0$ invariant mass distribution spectra (presented by histograms) measured by Ballam *et al* [2]. In this figure, the calculated cross-section is normalized to the measured spectrum at the peak. The sharp peak appearing in the calculated spectrum at $\sim$ 782 MeV is the characteristic feature of $\omega$-meson. The calculated spectra, as shown in this figure, reproduce well the respective peak positions of all measured distributions.

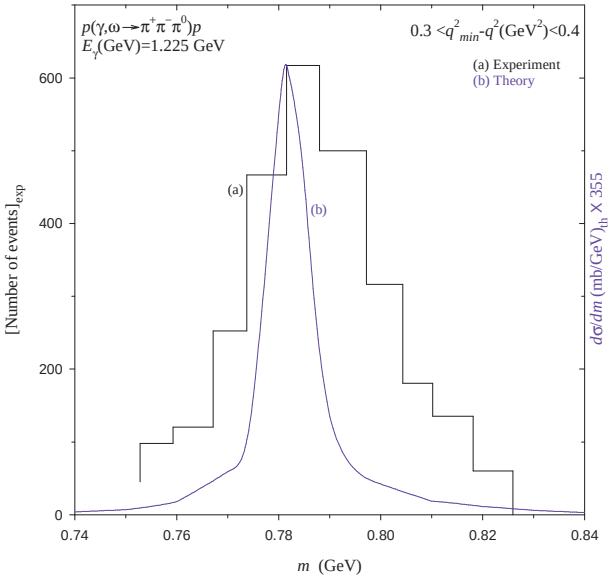


**Figure 5.** The calculated $\omega(\rightarrow \pi^+\pi^-\pi^0)$ meson mass distribution spectrum is compared with the data due to SAPHIR Collaboration [19]. The histogram (a) represents the measured number of events for the $\pi^+\pi^-\pi^0$ invariant mass distribution spectrum [19]. The solid curve (b) corresponds to the calculated cross-section ($\mathrm{d}\sigma/\mathrm{d}m$ in eq. (1)), normalized to the peak of the measured distribution.

These agreements elucidate the production of the $\omega$-meson in the intermediate state. The mismatch in widths between the calculated and the measured spectra (even in other figures also) may be due to the resolution width associated with the detector. The calculated cross-section at the peak is increased to $\sim$10.51 mb/GeV at $E_\gamma = 9.3$ GeV from 7.25 mb/GeV at $E_\gamma = 2.8$ GeV.

We present in figure 3 the calculated cross-section, i.e., $\mathrm{d}\sigma/\mathrm{d}m$ due to eq. (10), along with the data for $\pi^+\pi^-\pi^0$ invariant mass distribution in the energy bins: $E_\gamma$ (in GeV) = 1.1–1.5; 1.5–1.8; 1.8–2.5 and 2.5–6.0. In this figure, the histograms represent the $\pi^+\pi^-\pi^0$ invariant mass distribution spectra measured by the BUBBLE chamber group [3]. The dashed curves describe the phase-space distributions (see in ref. [3]). The solid curve in each energy bin is obtained by multiplying the calculated cross-section by a normalizing factor and adding it with the respective phase space (dashed curve). The normalizing factors are found to be 14.5, 2.9, 3.4 and 3.2 for the beam energy ($E_\gamma$) bin: 1.1–1.5 GeV, 1.5–1.8 GeV, 1.8–2.5 GeV and 2.5–6 GeV respectively. This figure shows that the calculated result reproduces the peak position in each energy bin. The actual magnitudes of the calculated cross-sections are presented in figure 4. This figure shows that the peak cross-section is enhanced to $\sim$7.73 mb/GeV at $E_\gamma$(GeV) = 2.5–6.0 from $\sim$2.31 mb/GeV at $E_\gamma$(GeV) = 1.1–1.5.

Recently, the SAPHIR Collaboration measured the $\pi^+\pi^-\pi^0$ invariant mass distribution spectrum in the energy bin: $1.2 < E_\gamma(\mathrm{GeV}) < 1.25$ with an additional

constraint: $0.3 < q^2_{\min} - q^2(\mathrm{GeV}^2) < 0.4$ [19]. Since the variation in the beam energy $E_\gamma$ is negligibly small (less than 50 MeV) when compared with the energy in the bin, we calculate $\mathrm{d}\sigma/\mathrm{d}m$ using eq. (1) at $E_\gamma = 1.225$ GeV for this spectrum. We compare the calculated result with the measured spectrum (stated above) in figure 5. In this figure, the measured distribution is shown by the histogram whereas the solid curve represents the calculated spectrum (normalized to the peak of the measured distribution). The magnitude of the calculated cross-section at the peak is about 1.7 mb/GeV. In this case also, the calculated result is in good agreement with the measured distribution.

## 4. Conclusions

The differential cross-section for the $\pi^+\pi^-\pi^0$ invariant mass distribution in the $\gamma p$ reaction in the GeV region is calculated. Since the $\omega$-meson couples strongly to $\pi^+\pi^-\pi^0$ in this energy region, we consider that this event in the final state arises due to the decay of the $\omega$-meson produced in the intermediate state. The agreement between the calculated and the measured peak positions corroborates this consideration. The reaction amplitude $f_{\gamma p\to\omega p}$, which is extracted from the latest $\omega$-meson photoproduction data, is used to estimate the magnitude of the cross-section. Other factors in this calculation are evaluated using the well-known procedure for them. Therefore, our calculation gives reliable cross-section for the $\pi^+\pi^-\pi^0$ invariant mass distribution in the $\gamma p$ reaction.

## Acknowledgements

The author gratefully acknowledges A K Mohanty, R K Choudhury and S Kailas.

## References

[1] Aachen-Berlin-Bonn-Hamburg-Heidelberg-München Collaboration, *Phys. Rev.* **175**, 1669 (1968)
M Davier *et al*, *Phys. Rev.* **D01**, 790 (1970)
Y Eisenberg *et al*, *Phys. Lett.* **B34**, 439 (1971)
[2] J Ballam, *et al*, *Phys. Rev.* **D07**, 3150 (1973)
[3] Brown-Harvard-MIT-Padova-Weizmann Institute Bubble Chamber Group, *Phys. Rev.* **155**, 1468 (1967)
[4] T H Bauer, R D Spital, D R Yennie and F M Pipkin, *Rev. Mod. Phys.* **50**, 261 (1978)
D R Yennie, *ibid.* **47**, 311 (1975)
[5] H B O'Connell, B C Pearce, A W Thomas and A G Williams, *Prog. Part. Nucl. Phys.* **39**, 201 (1997)
[6] J J Sakurai, *Currents and mesons* (The University of Chicago Press, Chicago and London, 1969) p. 48
R K Bhadury, *Models of the nucleon* (Addison-Wesley Publishing Company, Inc., New York and Singapore, 1988) p. 261

[7] G M Huber *et al*, *Phys. Rev.* **C68**, 065202 (2003)
G M Huber, G J Lolos and Z Papandreou, *Phys. Rev. Lett.* **80**, 5285 (1998)
G J Lolos *et al*, *ibid.* **80**, 241 (1998)
[8] R Koniuk, *Nucl. Phys.* **B195**, 452 (1982)
S Capstick CEBAF-TH-93-18
S Capstick and W Roberts, nucl-th/0008028
S Capstick, *Phys. Rev.* **D46**, 2864 (1992)
S Capstick and W Roberts, *Phys. Rev.* **D49**, 4570 (1994)
[9] Donald H Perkins, *Introduction to high energy physics*, second edition (Addison-Wesley Publishing Company, London and Tokyo, 1982) p. 180
[10] P Jain, B Pire and J P Ralston, *Phys. Rep.* **271**, 67 (1996)
[11] CBELSA/TAPS Collaboration: D Trnka *et al*, *Phys. Rev. Lett.* **94**, 192303 (2005)
[12] Swapan Das, *Phys. Rev.* **C78**, 045210 (2008)
[13] J J Sakurai, *Phys. Rev. Lett.* **8**, 300 (1962)
[14] Particle Data Group, *Phys. Rev.* **D54**, 334 (1996)
[15] J A Gómez Tejedor and E Oset, *Nucl. Phys.* **A600**, 413 (1996)
G I Lykasov, W Cassing, A Sibirtsev and M V Rzjanin, *Eur. Phys. J.* **A6**, 71 (1999)
M Gourdin, in *Meson resonance and related phenomena* edited by R H Dalitz and A Zichichi (Editrice Compositori Publishers, Bologna, Italy, 1972) p. 219
[16] A Pautz and G Shaw, *Phys. Rev.* **C57**, 2648 (1998)
[17] A Sibirtsev, H-W Hammer, U-G Meißner and A W Thomas, *Eur. Phys. J.* **A29**, 209 (2006)
[18] A Sibirtsev, K Tsushima and S Krewald, nucl-th/0202083; *Phys. Rev.* **C67**, 055201 (2003)
[19] J Barth *et al*, *Eur. Phys. J.* **A18**, 117 (2003)
[20] W J Schwille, F J Klein, F Klein and J Barth (private communication)
Particle Data Group, *Phys. Lett.* **B667**, 340 (2008)
[21] M Kaskulov, E Hernandez and E Oset, nucl-th/0610067; *Eur. Phys. J.* **A31**, 245 (2007)